International Journal of Autonomous Robotics and Intelligent Systems
Vol. 1, No. 1, June 2025 [117-128]

Development of 3-Phase Power Measurement Instrument

Ku Muhammad Muslih Bin Ku Ahmad Bistamam[1], Mohd Nasir Ayob[1*], Hassrizal Hassan Basri[1], Muhamad Safwan Muhamad Azmi[2], Siti Marhainis Othman[1], Mohd Sani Mohamad Hashim[2]

[1]Dept. of Mechatronics, Faculty of Electrical Engineering & Technology, Universiti Malaysia Perlis
[2]Dept. of Mechanical, Faculty of Mechanical Engineering & Technology, Universiti Malaysia Perlis

Received 8 July 2025, Revised 16 July 2025, Accepted 18 July 2025

ABSTRACT

This paper presents a real-time 3-phase power measurement instrument development using the ESP32 microcontroller and analog sensors. The instrument measures key electrical parameters including RMS voltage and current, real power, apparent power, reactive power and power factor for each phase of a 3-phase system. Key components used include the ZMPT101B voltage sensor, ACS712 current sensor, a 20x4 I2C LCD display and push buttons for manual data navigation. The system implements time-domain sampling and cross-correlation techniques for accurate phase angle and power factor calculations. The performance evaluation demonstrates its accuracy suitable for educational applications, as the measurement error compared to reference instruments was less than 2%.

Keywords: 3-Phase Power, Apparent Power, ESP32, Power Factor, Reactive Power, Real-time Monitoring

1. INTRODUCTION

The growing demand for energy efficiency and monitoring systems has led to an increase interest in accurate, low-cost power measurement tools. Traditional energy meters provide limited insights into power quality and are often expensive for detailed 3-phase analysis [1], as shown in Figure 1. Thus, this project aims to develop a microcontroller-based 3-phase power measurement instrument that able to provide real-time data for all key electrical parameters, using affordable sensors and open-source platforms [2]. The system is intended for educational and light industrial usage, with balancing cost, complexity and measurement fidelity.

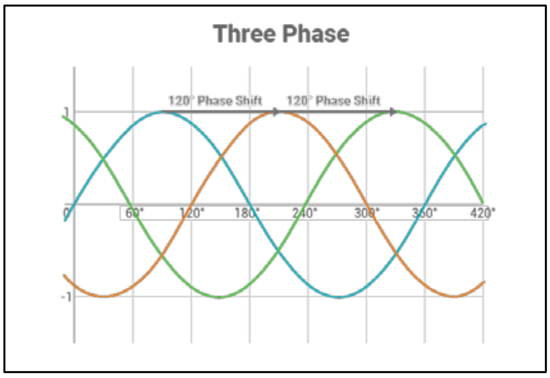

Figure 1. 3-phase power system

*nasirayob@unimap.edu.my

Several studies and commercial systems have addressed power measurement techniques, particularly in the context of 3-phase systems [1][3]. Smart energy meters by utility companies generally use digital signal processing to measure energy consumption with high accuracy [4][5]. However, these meters are closed-source, expensive, and often limited to cumulative energy data rather than real-time parameters [6].

Research into microcontroller-based power measurement systems, such as those using Arduino and ESP32, has demonstrated that accurate real-time monitoring is feasible using appropriate analog sensors and algorithms [7][8]. The ZMPT101B sensor is commonly used for voltage measurement due to its isolation and linearity, while the ACS712 sensor is preferred for current sensing because of its low cost and ease of integration. Several open-source projects and academic prototypes have shown that RMS values, active and reactive power, and power factor can be derived through synchronous sampling and mathematical processing [9]. Cross-correlation methods for phase angle detection have been proven effective in digital signal processing literature [10][11], especially when implemented with high-resolution sampling and filtering. For example, M.H. Rashid [1] discusses the viability of digital approaches for power measurement, especially when constrained by resource-limited embedded platforms [12][13].

Despite these advances, most implementations focus on single-phase systems. There is a noticeable gap in accessible, low-cost, open-source 3-phase meters that support comprehensive real-time monitoring and data logging [14]. This project addresses that gap by integrating multiple sensing and processing techniques into a unified system using affordable microcontrollers and sensors.

2. MATERIAL AND METHODS

2.1 Hardware Design

The system is centered around the ESP32 microcontroller, chosen for its dual-core processing, integrated Wi-Fi/Bluetooth, and multiple ADC channels. Voltage sensing is accomplished using three ZMPT101B modules, each connected to a phase. These modules provide analog output proportional to the input AC voltage, which is then sampled by the ESP32. Current is measured using three ACS712 (5A) sensors, each providing analog voltage outputs corresponding to the load current.

A 20x4 I2C LCD is used for output display, connected via I2C to reduce pin usage. Four push buttons are included for user input: one each for voltage, current, power (cycled through real/apparent/reactive) and power factor. Debouncing is handled in software to ensure reliable operation.

Power is supplied via USB or a regulated 5V adapter. Each sensor circuit is designed with proper biasing and filtering to ensure linearity and reduce noise. Figure 2 shows the completed instrument box, while Figure 3 illustrates the internal wiring, including sensors, a microcontroller, power supply units, and a display.

Figure 2. The 3-phase power measurement instrument

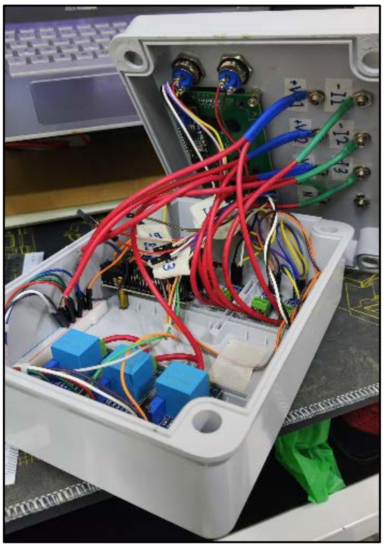

Figure 3. The internal of the 3-phase power measurement instrument

2.2 Firmware and Signal Processing

The firmware is developed using the Arduino IDE with libraries for LCD, I2C communication and button debouncing. The ESP32 samples voltage and current synchronously using ADC channels. Each waveform is sampled over one or more full cycles (depending on sample window size). RMS values are calculated using Equation (1) and (2), while apparent power is calculated using Equation (3):

$$V_{rms} = \sqrt{\frac{1}{N}\sum_{i=1}^{N} V_i^2} \tag{1}$$

$$I_{rms} = \sqrt{\frac{1}{N}\sum_{i=1}^{N} I_i^2} \tag{2}$$

$$S = \frac{1}{N}\sum_{i=1}^{N} V_i \cdot I_i \tag{3}$$

Real power is derived as in Equation (4), and reactive power is calculated using the Pythagorean theorem as in Equation (5):

$$P = V_{rms} \cdot I_{rms} \cdot cos\,\varphi \tag{4}$$

$$Q = V_{rms} \cdot I_{rms} \cdot sin\,\varphi \tag{5}$$

Phase angle and power factor are computed using cross-correlation between voltage and current signals to determine the time lag. The lag is converted to angle using the sampling frequency and waveform period, and power factor is then derived as in Equation (6):

$$PF = |cos\,\varphi| \tag{6}$$

The LCD display shows 6 different pages for 6 different parameters for all phase that the instrument reads and calculate, as shown in Figure 4. The pages are toggled when the button are pressed. The third button can be used to toggle the display for 3 types of power (real, apparent and reactive). Data is also sent via serial in CSV format for logging or remote processing.

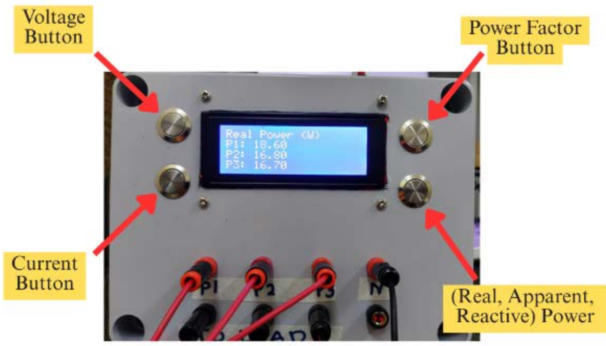

Figure 4. Instrument's button placement

The system operates through four key processes: data acquisition, processing, communication, and monitoring. Voltage and current signals from each phase are captured by sensors and conditioned before being sampled by the ESP32 microcontroller. The microcontroller computes electrical parameters such as RMS values, power factor, active, reactive and apparent power, as well as phase imbalance. Processed data is displayed on an LCD and optionally transmitted to an IoT platform for real-time monitoring or stored locally for offline analysis. A visual summary is shown in the block diagram in Figure 5.

International Journal of Autonomous Robotics and Intelligent Systems
Vol. 1, No. 1, June 2025 [117-128]

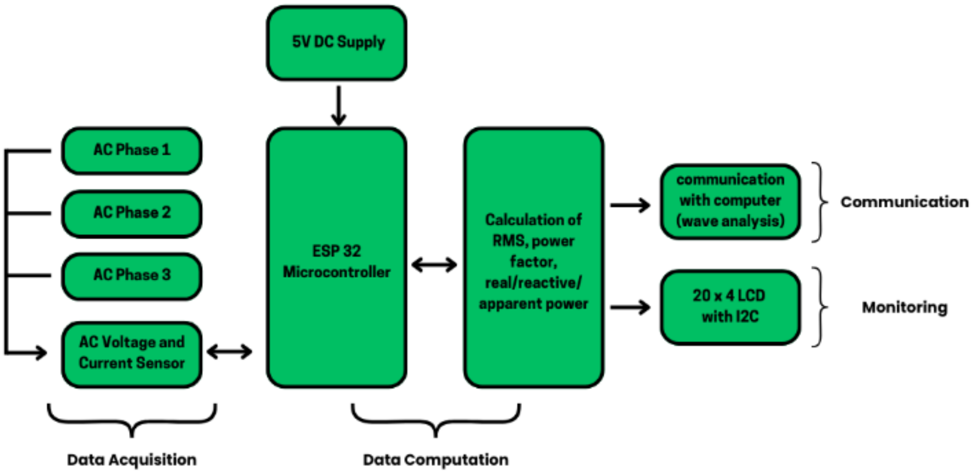

Figure 5. System's block diagram

3. RESULTS AND VALIDATION

3.1 Output Metrics

The system successfully measures and displays the following parameters, including per-phase V_{rms} and I_{rms}, real, apparent and reactive power, as well as power factor for each phase. The LCD updates in real-time and provides a clear layout of the selected metrics. Simultaneously, the ESP32 outputs the data via the serial monitor in real time as shown in Figure 6, formatted as complete CSV lines containing all per-phase and total values. This data can be monitored directly on a connected PC using the Arduino Serial Monitor. The serial monitor shows the readings of mentioned parameter for each phase while connecting to voltage supply and load (light bulb).

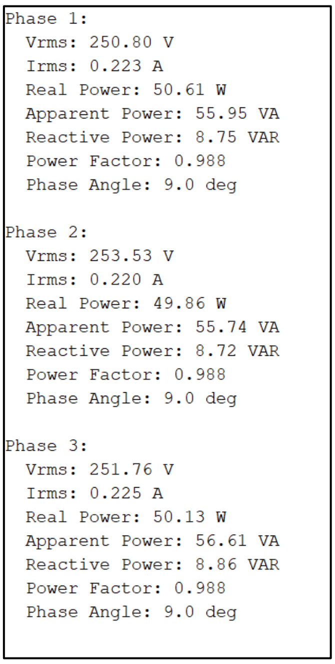

```
Phase 1:
  Vrms: 250.80 V
  Irms: 0.223 A
  Real Power: 50.61 W
  Apparent Power: 55.95 VA
  Reactive Power: 8.75 VAR
  Power Factor: 0.988
  Phase Angle: 9.0 deg

Phase 2:
  Vrms: 253.53 V
  Irms: 0.220 A
  Real Power: 49.86 W
  Apparent Power: 55.74 VA
  Reactive Power: 8.72 VAR
  Power Factor: 0.988
  Phase Angle: 9.0 deg

Phase 3:
  Vrms: 251.76 V
  Irms: 0.225 A
  Real Power: 50.13 W
  Apparent Power: 56.61 VA
  Reactive Power: 8.86 VAR
  Power Factor: 0.988
  Phase Angle: 9.0 deg
```

Figure 6. Instrument's readings on serial monitor

3.2 Accuracy and Stability Testing

To evaluate the stability and performance of the 3e-phase power measurement instrument, a one-minute data collection session was conducted for each individual phase under constant resistive load. The data were recorded and visualized through time-based graphs. This analysis assessed parameter consistency over time and the reliability of the instrument in continuous operation. Table 1 shows the analysis of the electrical parameter during one minute data collection.

Table 1 Analysis of electrical parameter

Parameter	Phase	Mean	Min	Max	Range	Std. Dev.
Voltage (V)	1	248.84	242.63	252.47	9.84	1.592
	2	250.78	247.69	253.74	9.84	0.866
	3	250.77	248.59	251.48	9.84	0.383
Current (A)	1	0.224	0.214	0.227	0.013	0.002
	2	0.217	0.212	0.220	0.013	0.001
	3	0.219	0.217	0.221	0.013	0.001
Real Power (W)	1	50.24	47.02	51.52	4.50	0.724
	2	48.15	46.72	49.86	4.50	0.499
	3	49.26	47.98	49.99	4.50	0.261
Apparent Power (VA)	1	55.84	53.15	57.19	4.04	0.642
	2	54.31	53.04	55.74	4.04	0.370
	3	54.90	54.26	55.48	4.04	0.175
Reactive Power (VAR)	1	8.73	8.31	8.94	0.63	0.099
	2	8.50	8.30	8.72	0.63	0.057
	3	8.58	8.49	8.68	0.63	0.028
Power Factor	1	0.988	0.988	0.988	0.000	3E−16
	2	0.988	0.988	0.988	0.000	3E−16
	3	0.988	0.988	0.988	0.000	3E−16

These results confirm that the instrument maintains excellent stability in measuring voltage, current and power characteristics over time. Graphical analysis supports this with near-constant traces across all parameters as shown in Figure 7.

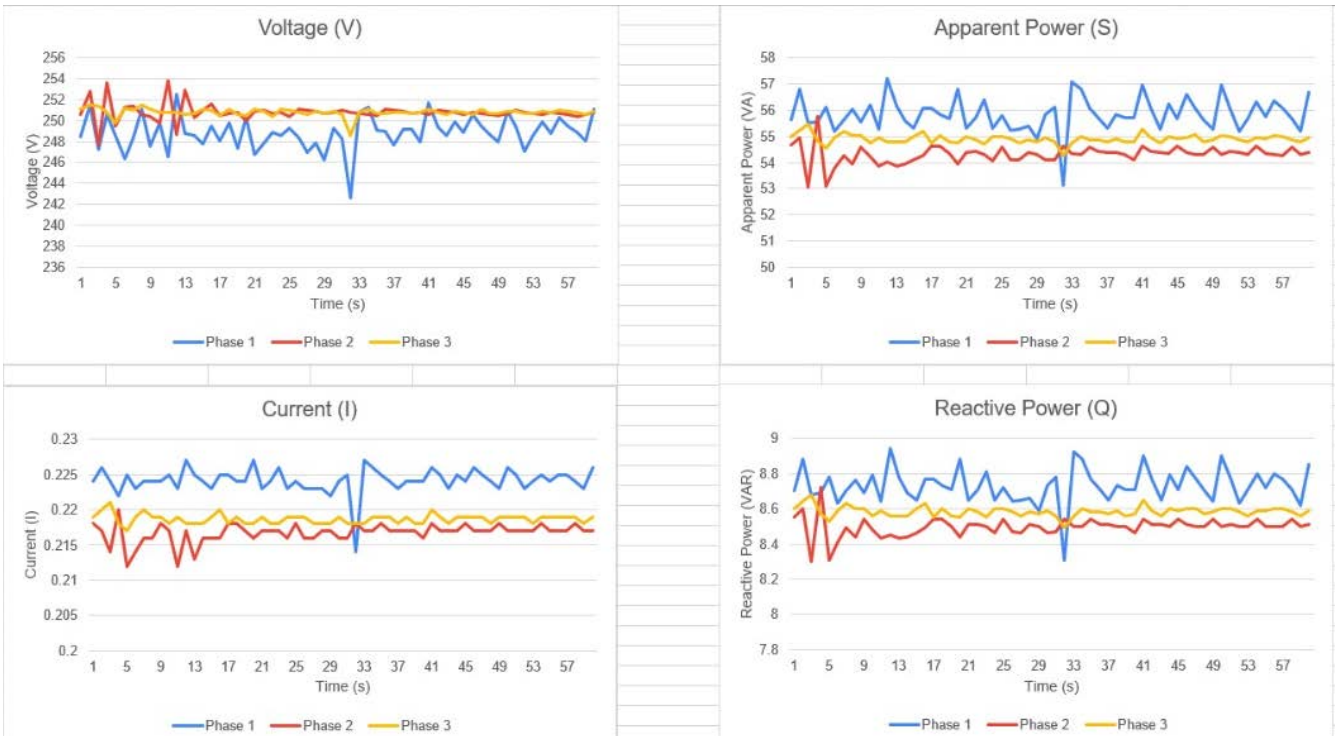

Figure 7. Sample of time series data from voltage and current measurement, and calculated instantaneous power component

3.3 Measurement Comparison

The system was rigorously tested under various load conditions and compared against a calibrated commercial digital power meter to assess accuracy and operational stability. Voltage and current measurements from the ESP32 system showed a deviation of less than ±5% from the reference meter, which is acceptable for non-industrial, real-time monitoring applications.

Under no-load conditions where only the motor-generator set was active, the system accurately captured baseline voltage and current. Voltage errors were low: 0.769% (Phase 1), 0.088% (Phase 2) and 0.092% (Phase 3). Small current values (0.168 A, 0.167 A, 0.172 A) were measured due to internal motor operation, with acceptable errors of 0.592%, 1.183% and 1.775% respectively.

With one resistive bulb, the instrument recorded voltage readings of 242.5 V, 245.3 V and 245.1 V (Phases 1–3), closely matching the reference 244 V, yielding errors of 0.614%, 0.532% and 0.450%. Current readings were 0.294 A, 0.298 A and 0.297 A, against a reference of 0.300 A, with percentage errors of 2%, 0.667% and 1% respectively.

Under increased load with two bulbs, voltage readings were 245.5 V, 244.5 V and 244.7 V, compared to reference values of 243 V, 244 V, and 242 V. Errors were 1.029%, 0.205% and 1.116%. Current values measured were 0.425 A, 0.427 A and 0.428 A (vs. 0.430 A), with respective errors of 1.163%, 0.698% and 0.465%.

Voltage recorded was 243.3 V, 242.7 V and 243.5 V, compared to 241 V (Phases 1 & 3) and 242 V (Phase 2). Errors remained low at 0.954%, 0.289% and 1.037%. Current values were 0.550 A, 0.556 A and 0.558 A versus 0.559 A reference, with percentage errors of 1.610%, 0.537% and 0.179%. With four bulbs, voltage readings were 244.6 V, 246.2 V and 245.7 V, compared to 244 V reference, giving errors of 0.246%, 0.902% and 0.697%. Current values were 0.690 A, 0.688 A and 0.687 A, versus 0.689 A across phases, yielding very low errors of 0.145%, 0.145% and 0.290%.

These results confirm the instrument's accuracy and robustness under both minimal and high-load conditions, making it suitable for lab and educational settings. The system was rigorously tested under various load conditions and compared against a calibrated commercial digital power meter to assess accuracy and operational stability. Voltage and current measurements from the ESP32 system showed a deviation of less than ±5% from the reference meter, which is acceptable for non-industrial, real-time monitoring applications. Table 2 summarizes the measured voltage and current accuracy across five load scenarios.

Table 2 Summary of voltage and current comparison

Load Condition	Phase	Voltage (V)	Ref Voltage (V)	Error (%)	Current (A)	Ref Current (A)	Error (%)
No Load	1	239.8	Ref	0.769	0.168	Ref	0.592
	2	248.8	Ref	0.088	0.167	Ref	1.183
	3	248.8	Ref	0.092	0.172	Ref	1.775
1 Bulb	1	242.5	244	0.614	0.294	0.300	2.000
	2	245.3	244	0.532	0.298	0.300	0.667
	3	245.1	244	0.450	0.297	0.300	1.000
2 Bulbs	1	245.5	243	1.029	0.425	0.430	1.163
	2	244.5	244	0.205	0.427	0.430	0.698
	3	244.7	242	1.116	0.428	0.430	0.465
3 Bulbs	1	243.3	241	0.954	0.550	0.559	1.610
	2	242.7	242	0.289	0.556	0.559	0.537
	3	243.5	241	1.037	0.558	0.559	0.179
4 Bulbs	1	244.6	244	0.246	0.690	0.689	0.145
	2	246.2	244	0.902	0.688	0.689	0.145
	3	245.7	244	0.697	0.687	0.689	0.290

3.4 Power Management Comparison

A total input power comparison was conducted between the developed 3-phase measurement instrument and a calibrated reference device under varying resistive loads (0 to 4 bulbs). The developed instrument demonstrated high accuracy at all load levels. The comparison can be observed in Table 3.

Table 3 Total input power

Measurement	Instrument Input Power	Reference Instrument Input Power	Error (%)
0 Bulb	123.03 W	122.90 W	0.106
1 Bulb	214.58 W	216.96 W	1.097
2 Bulb	309.71 W	309.71 W	0.000
3 Bulb	399.77 W	399.85W	0.020
4 Bulb	500.87 W	498.30 W	0.515

Figure 8 illustrates the relationship between the number of connected light bulb loads and the corresponding total input power readings recorded by both the developed instrument and the reference instrument. The graph reveals a clear linear trend for both sets of measurements, indicating that input power increases proportionally with the number of bulbs connected. This linearity confirms the correct functional behavior of both instruments in response to varying loads. The smooth, incremental increase in power across all load levels reflects the system's reliability and stability during testing.

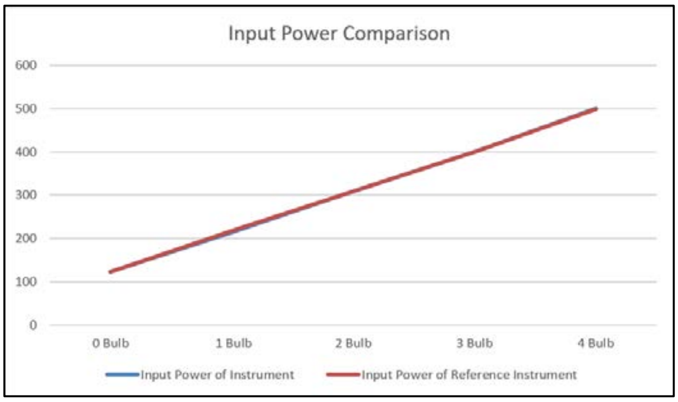

Figure 8. Input power comparison

Table 4 and Figure 9 present a comparison between the output power measured by the developed instrument and reference calculations for Phase 1 under varying load conditions. At no-load, the device recorded 37.74 W, closely matching the reference value of 38.36 W with a 1.62% error, representing baseline excitation power required to sustain the generator's magnetic field.

As additional bulbs were connected, the measured output power increased proportionally, and the instrument tracked these changes accurately with all errors remaining below 2%. The smallest deviation (0.19%) occurred at the three-bulb load, indicating optimal operating conditions for measurement stability.

Notably, the curve in the figure is not strictly linear. This non-linearity is expected in practical generator-based systems. At zero load, a significant portion of the power is consumed by the generator's excitation system to maintain the rotating magnetic field. As load increases, this excitation power becomes proportionally smaller relative to total output, causing a nonlinear scaling effect. Furthermore, the drop in measured output power at four bulbs may be attributed to voltage sag under higher load, slight generator inefficiency, or dynamic regulation of field strength, all of which are common in small-scale synchronous generator setups.

These results confirm the accuracy and responsiveness of the measurement instrument, as well as its ability to reflect real-world power behavior in electromechanical systems.

Table 4 Total output power

Measurement	Instrument Output Power	Reference Instrument Output Power	Error (%)
0 Bulb	37.74 W	38.36 W	1.62
1 Bulb	49.75 W	48.85 W	1.84
2 Bulb	76.49 W	77.15 W	0.85
3 Bulb	82.82 W	82.66 W	0.19
4 Bulb	63.11 W	61.97 W	1.84

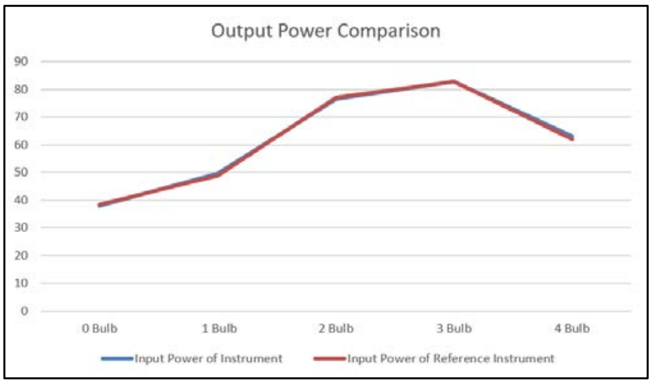

Figure 9. Output power comparison

4. DISCUSSION

The developed instrument offers an effective balance between cost and performance, making it suitable for educational and light industrial use. The use of time-domain cross-correlation for phase angle detection has proven to be a practical and computationally efficient approach, although it is sensitive to signal noise and limited by the resolution of the onboard ADC. Accurate measurements are highly dependent on the linearity and calibration of the voltage and current sensors.

The pushbutton-based user interface enables intuitive navigation of real-time measurements, while the serial output feature facilitates seamless data logging and integration with external analysis tools or microcontrollers.

However, the system does have limitations. The ACS712 current sensors used in this design are rated for 5A, which restricts the system's applicability in high-load environments. Additionally, the sensor exhibits reduced accuracy at low current levels due to inherent offset voltage, resulting in increased relative error.

5. CONCLUSION

A fully functional 3-phase power measurement instrument was developed, capable of accurately capturing and displaying key electrical parameters such as voltage, current, real power, reactive power and apparent power across all three phases. The system demonstrated reliable real-time monitoring via serial communication and was validated against a professional-grade reference device (SX48 digital meter), confirming its accuracy and suitability for academic and experimental use. The performance evaluation demonstrates accuracy suitable for educational applications, as the measurement error compared to reference instruments was less than 2%.

ACKNOWLEDGEMENTS

The author would like to extend sincere gratitude to everyone who contributed to the successful completion of this project. Special thanks to the Faculty of Electrical Engineering & Technology, UniMAP for providing the necessary resources and facilities to conduct the study.

REFERENCES

[1] A. R. Beig, 10 - Three-phase AC supply, in M. H. Rashid, Ed., *Electric Renewable Energy Systems*, Boston: Academic Press, 2016, pp. 183–208.
[2] J. A. Buck, W. H. Hayt, Engineering Electromagnetics. McGraw-Hill Education, 2011.
[3] A. Hannah, 2024. Case Studies in WYE & Delta Distribution Capacitor Installations. In 2024 IEEE Rural Electric Power Conference (REPC), pp. 14–21.
[4] F. Sánchez-Sutil, A. Cano-Ortega, 2021. Design and testing of a power analyzer monitor and programming device in industries with a lora lpwan network, Electronics (Switzerland), vol. 10, no. 4, pp. 1–37.
[5] J. Mikulović, T. Šekara, M. Forcan, 2023. Power definitions for three-phase systems in terms of instantaneous symmetrical components, International Journal of Electrical Power & Energy Systems, vol. 147, p. 108808.
[6] A. E. Emanuel, 1998. The Buchholz-Goodhue apparent power definition: the practical approach for nonsinusoidal and unbalanced systems, IEEE Transactions on Power Delivery, vol. 13, no. 2, pp. 344–350.
[7] I. Nevliudov, V. Yevsieiev, S. Maksymova, N. Demska, N. Starodubcev, O. Klymenko, 2023. Monitoring System Development for Equipment Upgrade for IIoT. In 2023 IEEE 5th International Conference on Modern Electrical and Energy System (MEES), pp. 1–5.
[8] M. A. S. M. Dzahir, K. S. Chia, 2023. Evaluating the Energy Consumption of ESP32 Microcontroller for Real-Time MQTT IoT-Based Monitoring System. In 2023 International Conference on Innovation and Intelligence for Informatics, Computing, and Technologies (3ICT), pp. 255–261.
[9] P. M. Tzvetkov, K. S. Galabov, 2022. True RMS Ammeter Calibration by Using Standard Square Waveform Signal and Algorithm for Measurement and Processing of Results. In 2022 XXXII International Scientific Symposium Metrology and Metrology Assurance (MMA), pp. 1–5.
[10] I. Tudosa, F. Picariello, P. Daponte, L. De Vito, S. Rapuano, N. G. Paulter, 2022. Prototype of high accuracy single input phase measurement instrument. Measurement, vol. 201, p. 111595.
[11] P. Daponte, L. De Vito, F. Picariello, S. Rapuano, I. Tudosa, 2023. Sensitivity assessment of a phase measurement method used in a waveform recorder traceable testing for ElectroShock Weapons (ESW). In 2023 IEEE International Workshop on Technologies for Defense and Security (TechDefense), pp. 245–250.
[12] P. Yan, G. Liu, R. Wang, B. Xia, J. Zhang, L. Yi, 2022. Development method and comparative analysis of measurement accuracy of new broadband and wide range current transformers. In 2022 4th International Conference on Electrical Engineering and Control Technologies (CEECT), pp. 379–384.
[13] M. Malengret, C. T. Gaunt, 2020. Active Currents, Power Factor, and Apparent Power for Practical Power Delivery Systems. IEEE Access, vol. 8, pp. 133095–133113.

[14] T. Vince, M. Sroka, B. Fecko, B. Peryvertailo, R. Yatsiuk, I. Anna, 2023. A Universal DSP Module for Simultaneous Multiple RS232 Communication with Synchronous Measurements Reading Capability. In 2023 IEEE 5th International Conference on Modern Electrical and Energy System (MEES), pp. 1–5.